Hydraulic conductivity predictive model of RHA-ameliorated laterite for solving landfill liner leachate, soil and water contamination and carbon emission problems

Kennedy C. Onyelowe[1,*], Ahmed M. Ebid[2], Jair de Jesús Arrieta Baldovino[3] and Michael E. Onyia[4]

[1]*Department of Civil Engineering, Kampala International University-Western Campus, Ggaba Road, Ishaka, Kampala, Uganda;* [2]*Department of Structural Engineering, Future University in Egypt, New Cairo, S Teseen, New Cairo 1, Cairo Governorate 11835, Egypt;* [3]*Department of Civil Engineering, Universidad de Cartagena, Cartagena de Indias 130015, Colombia;* [4]*Department of Civil Engineering, Faculty of Engineering, University of Nigeria, Nsukka, Nsukka-Onitsha Road, Nsukka, Enugu State, Nigeria*

Abstract

The environment is seriously being affected by the leachate release at the unconstructed and badly constructed waste containment or landfill facilities around the globe. The worst hit is the developing world where there is little or totally no waste management system and facilities to receive waste released into the atmosphere. This research work is focused on the leachate drain into the soil and the underground water from landfills, which toxicifies both the soil and the water. Also, the construction of the liner or barrier with cement poses serious threat to the environment due to oxides of carbon release and this research also took this into account by replacing the utilization of cement with rice husk ash (RHA), which has proven to have the potentials of replacing cement as a supplementary binder. Laboratory tests were conducted to determine the hydraulic conductivity (K) of lateritic soil (LS) ameliorated with different dosages of RHA. Other hydromechanical properties of the treated blend were studied and multiple data were generated for the artificial neural network (ANN) back-propagation (-BP), genetic algorithm (GA) and gradual reducing gradient (GRG), genetic programming (GP) and evolutionary polynomial regression (EPR) prediction exercises. Results show that the LS was a poorly graded A-2 sandy silt soil, which was subjected to three different compaction energies with the minimum of the British standard light (BSL) and derived k of 6.95E-10, 50.75E-10 and 32.33E-10 for BSL, west African standard and British standard heavy, respectively. The RHA addition improved the studied properties of the ameliorated LS. Out of the five models, the ANN-GRG outclassed others with a performance of 99% with minimal error compared with the rest. Potentially, this research has shown that RHA with a pozzolanic chemical moduli of 81.47% can replace cement in the construction of ecofriendly and more efficient landfills and waste containemnt barriers to save the soil and the underground water as well as the environment from leachate contamination and carbon emissions.

Keywords: environmental geotechnics; AI models; leachate contamination; sanitary landfill; RHA-ameliorated laterite (RHA-AL); soil permeability; carbon emission

*Corresponding author: kennedychibuzor@kiu.ac.ug, konyelowe@gmail.com

Received 17 April 2022; revised 2 June 2022; accepted 24 June 2022

International Journal of Low-Carbon Technologies 2022, 17, 1134–1144

https://doi.org/10.1093/ijlct/ctac077 Advance Access publication 25 July 2022

1 INTRODUCTION AND BACKGROUND

A landfill liner is a structure that forms a barrier between solid waste and the underlying soil and underground water. Rice husk ash (RHA)-ameliorated laterites are materials that can be employed for the protection of ground waters and surface waters surrounding landfill depositories because they produce low carbon emission operation. A considerable amount of practical experience and experimental understanding has been built upon using such materials. However, many uncertainties remain in their utilization as either the sole protector of the aquatic environment or in conjunction with proprietary lining materials. A major difficulty with using RHA-ameliorated laterites is the significant variation in permeability, compression index, swell index, liquid limit (LL) and percentage fines, which can occur with relatively small changes in other properties [7, 16, 28].

A change in moisture content of only 2% or 3% can result in a permeability variation of an order of magnitude or more [31]. So, the hydraulic conductivity of such structures is of great importance because the liner can sustain the prevention of leachate (toxic substances from decaying solid waste) from seeping through the structure and destroying the soil structure and the underground water [30]. In contrast to the group of water-proofing agents, some chemicals will increase the rate of water absorption. These include calcium chloride and sodium chloride. They are generally used as dust palliatives to improve road surfaces

A permeability of landfills foundations is usually specified as the overriding requirement for a fine soil or material lining. An RHA-laterite soil may have suitable material characteristics, but the variation of permeability with moisture content, degree of compaction and soil structure must also be considered [29, 33]. Acceptability relates to the excavation, handling, trafficability, conditioning and compaction of a material required to achieve the desired low permeability. It is now generally accepted that the physical properties of green geomaterials (e.g. soils) are controlled by the composition of the soil, especially the mineralogy, by the arrangement of the mineral particles (i.e. the soil structure) and by the sizes and forms of the soil particles (i.e. the texture) [32].

In practice, the leachate levels and thus hydraulic gradients in landfills are kept low by pumping from wells. In laboratory permeability tests, the hydraulic gradients are usually significantly higher than in practice for reasons of practical flow measurement. Material suitability relates to the material type and whether it could potentially form a low-permeability barrier [15]. In order to achieve this, it is usual to specify the use of RHA laterite with suitable material characteristics as defined by its plasticity, material variability and clay content [13, 17].

Laterite soils have high concentrations of sesquioxides (Fe_2O_3 and Al_2O_3). Because of the sesquioxide content, these soils may be effectively stabilized with small amounts of cement and lime or ashes derived from rice husk [18, 24]. The laterite soil type and its composition have been known to influence stabilization results. They obtained satisfactory stabilization results for significantly different genetic laterite soils with variable compositions and concluded that all laterite soils could be stabilized using 4–7% cement for base construction. The effect of curing temperatures and age on the strength gain of stabilized natural soil-cement is very well known. Adding cement into the soil increases the unconfined compressive strength and reduces the permeability of the compacted blends [8].

All fine sustainable materials (e.g. clays and laterites) have a finite permeability and potential to attenuate contaminants, and even with a well designed and constructed system, contaminant migration from landfills will occur, be it gradual. Leakage rates in the field are generally recognized as more significant than the design rates because the scale and structural defects are not wholly represented in laboratory testing (e.g. [13, 20, 25]). The acceptability of such escapes must be balanced against the potentially prohibitive cost of attempting perfect containment. Santos *et al.* [26] concluded that the liquids produced in the landfill can also affect the layer's integrity due to the low dielectric constants. When the organic liquid replaces the water in the soil pores, the double layer of the soil particle shrinks and can generate macropores or cracks that cause an increase in hydraulic conductivity. To ensure good performance, regulatory agencies mandate that compacted soil be designed to have a hydraulic conductivity of less than or equal 10^{-7} cm/s when used in hazardous, industrial and municipal solid waste disposal sites. The hydraulic performance of geomaterials for liners construction is also affected due to the internal erosion process that involves the movement of fine particles due to the existence of high hydraulic gradients [10, 12].

The essential cementing admixtures for natural soils include portland cement, lime, a mixture of lime and fly ash and sodium silicate. Recently, RHA was introduced in various studies to enhance the performance of natural soils (e.g. [9, 17, 24, 27]), which react with RHA-alumina and silica. This is a long-term reaction and one that results in more significant strengths if RHA-soil mixtures are cured for a while. The clay fractions in geomaterials as an RHA-soil are chiefly flake-shaped particles arranged in sheet-like patterns. The relative amount of the clay-size fraction in soils has a considerable influence on other geotechnical characteristics of soils. For this reason, the compaction layers must have good adhesion at their interface to avoid highly permeable zones and obtain a low overall hydraulic conductivity of the liner.

In landfills comprising predominantly domestic waste, the dissolved contaminants in the leachate are considered of prime concern. However, clays have the potential to adsorb cations and anions from leachate, particularly the ions of heavy metals. Clays are generally deemed net negatively charged and attract positively charged cations within an adsorbed layer on the particle surfaces, the so-called double layer. Studies have shown that various stabilization processes have considerable influence on the plasticity, density–moisture relation, swell and shrinkage, strength and stability, as well as on the durability and weathering characteristics of the laterite soils used for landfills (e.g. [14, 19, 23, 30])

Because the landfills are also structures protecting the environment from toxic leachate and emissions, the RHA is proposed as eco-friendly supplementary binders to achieve sustainable waste

Table 1. *Statistical analysis of collected database.*

	ED kN.m/m³	RHA %	Cc -	Cs -	LL %	F %	K E-10 m/s
			Training set				
Min.	375	0.00	0.01	0.01	41.77	40.72	4.58
Max.	2200	17.61	0.08	0.06	53.54	55.77	50.79
Avg.	1141	7.39	0.03	0.02	47.92	47.57	18.17
SD	749	5.36	0.02	0.01	2.91	3.91	11.92
VAR	0.66	0.73	0.69	0.46	0.06	0.08	0.66
			Validation set				
Min.	375	0.00	0.01	0.02	40.88	38.46	6.52
Max.	2200	16.64	0.07	0.05	53.08	50.29	47.00
Avg.	1394	10.12	0.03	0.03	48.21	44.24	17.23
SD	756	6.32	0.03	0.01	3.40	2.93	11.11
VAR	0.54	0.62	0.97	0.44	0.07	0.07	0.64

landfill liner construction. Therefore, in this paper, intelligent methods have been used to predict the hydraulic conductivity of the RHA-ameliorated laterite, considering compaction energy, RHA proportion, compression index, swelling index, LL and percentage fines as input parameters. The artificial neural network (ANN), evolutionary polynomial regression (EPR) and genetic programming (GP) intelligent techniques were employed to optimize the use of RHA laterite geomaterial for landfill liners.

2 MATERIALS AND METHODS

2.1 Materials preparation

Lateritic soil (LS) was collected from a depth of 1.2 m from a borrowpit located at Olokoro, Nigeria. Lumps were removed by soft tampering with rubber pestle and it was sundried for three and a half days. After preparation, the test soils were stored in sackbags for use. In a similar procedure, rice husks were collected from rice farms and local milling factories in Abakaliki, Nigeria, where the rural and suburban dwellers are rice farmers. The husks were sundried also but for 7 days due to the level of absorbed moisture in the husks. After the drying period, the husks were combusted in a controlled combustion model proposed by Onyelowe *et al.* [23] to derive RHA. This was sieved through 2.35 mm sieve and stored also in silo bags for use in the soil amelioration process. These materials were prepared in accordance with appropriate material standard [5].

2.2 Experimental methods

Preliminary experimental processes were performed on the test materials and these included sieve analysis, compaction, Atterberg limits, specific gravity, xray fluorescence and diffraction (XRF and XRD) and scanning electron microscopy (SEM) to enable proper characterization of the test materials. These tests were done with the appropriate codes in mind (British Standard (BS); [3, 5]). The RHA meeting the pozzolanic materials requirements according to ASTM C618 [2] and BS 8615-1 [4] was further utilized in various proportions as presented in Table 1 to ameliorate the the hydromechanical properties of the LS and hydraulic conductivity (K), compresion index (Cc), swell index (Cs), LL and fines percentage were observed under different compaction energy density (ED) with a minimum of the British standard light (BSL) energy. These stabilization procedure was conducted with the requirements of BS 1924 [6]. Multiple experimental results were generated represening the studied parameters of the ameliorated LS.

2.3 Experimental data and statistical analysis

From the multiple experimental results, 45 records were collected for experimentally tested samples of RHA-ameliorated laterite. Each record contains the following data:

- ED Compactive energy density (kN.m/m³): ED = 375 kN.m/m³ for BSL compactive energy;, ED = 1000 kN.m/m³ for West African Standard compactive energy; and ED = 2200 kN.m/m³ for British standard heavy compactive energy.
- RHA Rice husk ash dosage (%)
- Cc Compression Index
- Cs Swell Index
- LL Liquid limit (%)
- F Fines percentage (%)
- K Hydraulic conductivity for pre-consolidation pressure of 80kN/m² (m/s)

The collected records were divided into training set (36 records) and validation set (9 records). The Appendix includes the complete dataset, while Tables 1 and 2 summarize their statistical characteristics and the Pearson correlation matrix. Finally, Figure 1 shows the histograms for both inputs and outputs.

2.4 Research program plan

Five different Artificial Intelligent (AI) techniques were used to predict the characteristic compressive strength of concrete with recycled aggregates using the collected database. These techniques are GP, three models of ANN with different training algorithms and polynomial regression optimized using genetic algorithm (GA), which is known as 'evolutionary polynomial

Table 2. *Pearson correlation matrix.*

	ED	RHA	Cc	Cs	LL	F	K
ED	1.00						
RHA	0.01	1.00					
Cc	-0.48	-0.68	1.00				
Cs	-0.46	-0.17	0.47	1.00			
LL	0.06	0.46	-0.45	-0.39	1.00		
F	-0.21	-0.67	0.51	0.16	-0.36	1.00	
K	0.24	-0.31	0.03	-0.12	-0.10	0.16	1.00

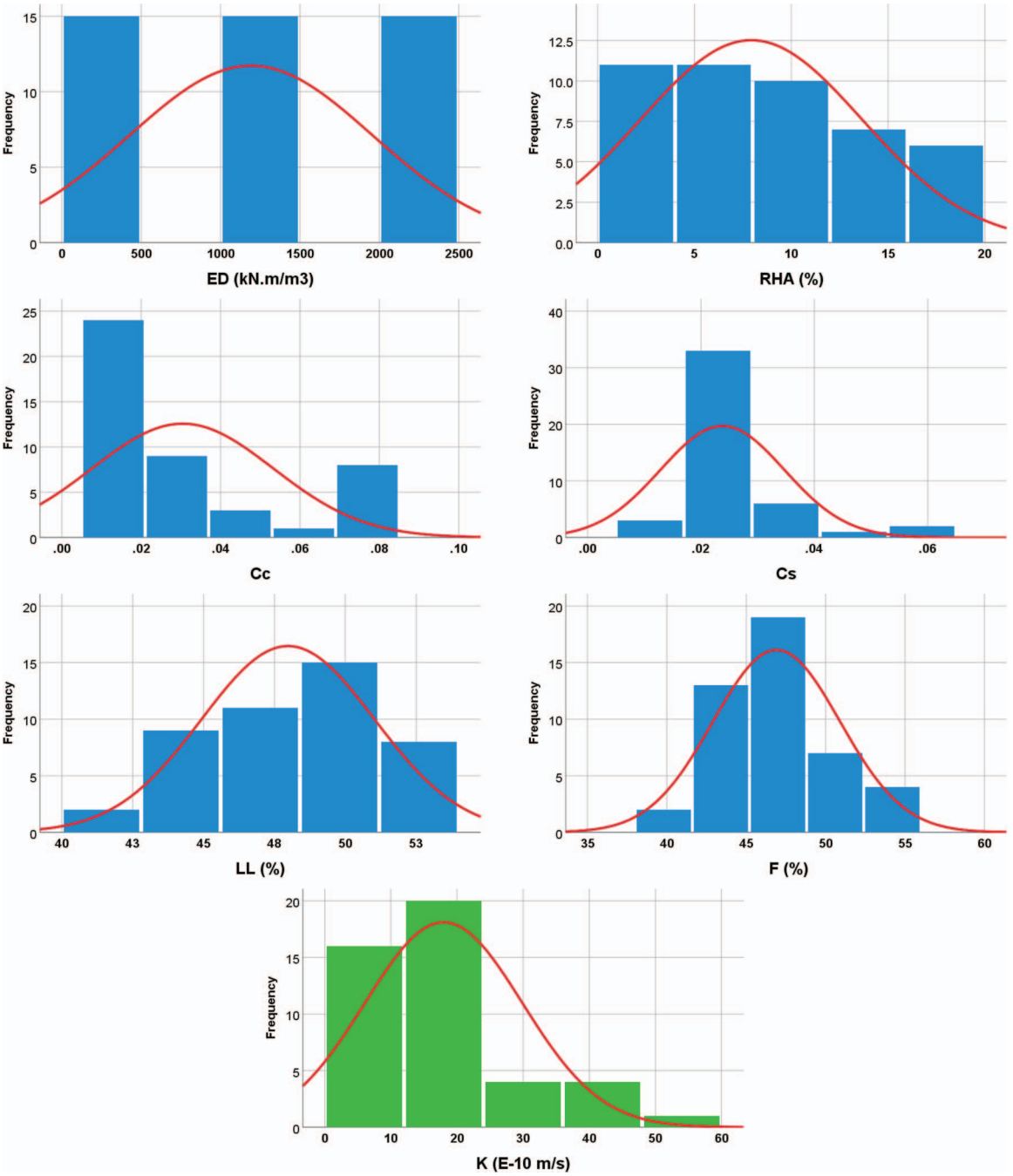

Figure 1. *Distribution histograms for inputs (in blue) and outputs (in green).*

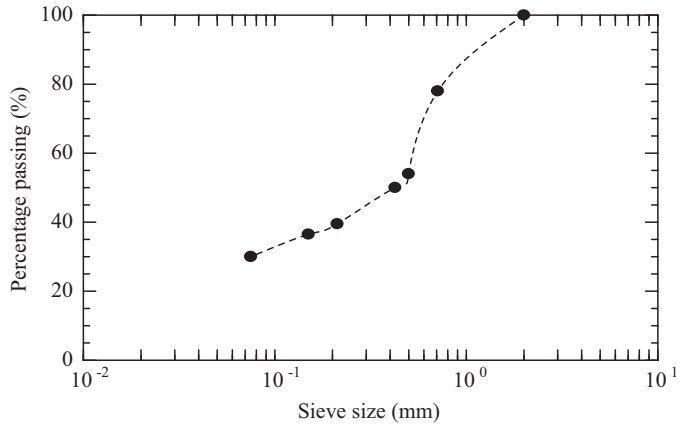

Figure 2. *Particle size analysis curve of the laterite.*

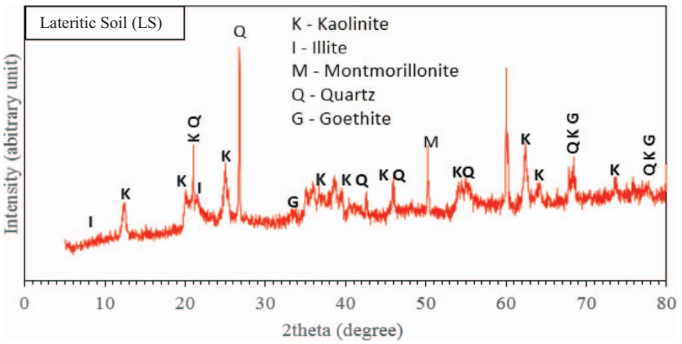

Figure 3. *XRD pattern of the untreated LS.*

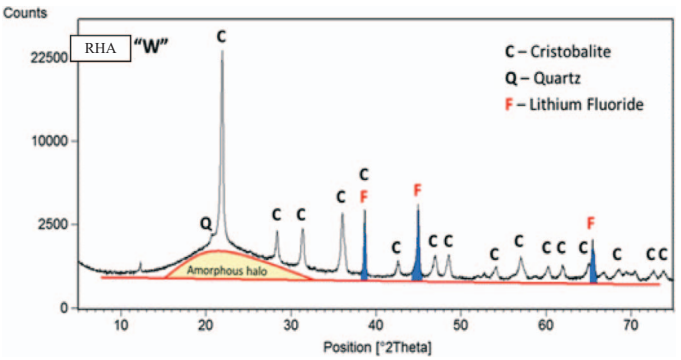

Figure 4. *XRD pattern of the RHA.*

regression' or EPR. All the three developed models were used to predict the hydraulic conductivity (K) in (m/s) using compactive ED in (kN.m/m³), RHA dosage (%), compression index (Cc), swell index (Cs), LL (%) and fines percentage (%) (F).

Each model on the three developed models was based on different approach (evolutionary approach for GP, mimicking biological neurons for ANN and optimized mathematical regression technique for EPR). However, for all developed models, prediction accuracy was evaluated in terms of sum of squared errors (SSE).

The following section discusses the results of each model. The accuracies of developed models were evaluated by comparing the SSE between predicted and calculated shear strength parameter values. The results of all developed models are summarized in Table 6.

3 RESULTS AND DISCUSSION

3.1 Materials characteristics

Figures 2, 3 and 4 show the gradation curve of the soil, XRD pattern of the untreated (non-ameliorated) soil and XRD pattern of the RHA, respectively. Tables 3, 4 and 5 show the summary of the basic properties, chemical oxide composition and pozzolanic chemical moduli (PCM), respectively, of the soil and RHA. Figure 2 shows poor gradation of the soil with 30% passing sieve number 200 as also presented in Table 3.

As presented in Figures 3 and 4, the x-ray diffraction patterns for the un-ameliorated LS in its natural state indicated a content of kaolinite minerals ($Al_2Si_2O_5(OH)_4$) for several 2theta = 12.5°, 26° and 51° dominating the soil and mixed deposit of marginal crystalline segments of silica (SiO_2) signified as goethite and quartz (FeO(OH)) found in blended kaolinite layers. 'Quite a number of studies for pronominally kaolinite mineral have shown varying 2theta' [1]. Onyelowe *et al.* [21] reported similar results with 2theta existing from 12.1° to 39.5°. Very little trace of illite in the group of mica-phyllosilicates and composition repeating measures of the pattern $(K,H_3O)Al,Mg,Fe)_2(Si,Al)_4O_{10}[(OH)_2.(H_2O)]$ at 2theta = 8.5°, 23° and 42.5° and montmorillonite ($Al_2H_2O_{12}Si_4$) seen at 2theta = 17.5°, 27.5°, 35°, 54.4° and 61.7° in blended sheet coatings were equally observed. The presence of these minerals (illite and montmorillonite) is responsible for the hydraulic conduction instability of the soil, which revealed a characteristic permeability behavior in waste containment structures. The RHA XRD pattern is dominated by cristobalite, which is a mineral polymorph of silica that is formed at very high temperatures as shown in Figure 4. It has a specific gravity range of 2.32–2.36, with uniaxial optical properties. Cristobalite can be found in the ashes of volcanic eruptions and in some bentonite clays, which gives the ash in which is dominated the pozzolanic ability as shown subsequently in Tables 4 and 5. The second dominating compound in the RHA XRD pattern is the lithium fluoride, which has a high density of 6.51 g/cm³ and reacts vigorously with a high melting point of 2310 C and very insignificant coefficient of thermal expansion of 37E-6/ °C. This behavior also gives the RHA the advantaged potential it exhibits as a supplementary cementitous binder in soil stabilization procedures. In Table 3, the soil has a maximum dry density of 2.45 g/cm³ obtained at optimum moisture of 17%, specific gravity of 2.21 and an LL of 35% and has 30% passing sieve number 200, which classifies the soil as poorly graded A-2 sandy silt soil according to AASHTO and US classification systems. The initial hydraulic conductivity (K) of the non-ameliorated LS at 375 kN.m/m³ compaction energy recorded 6.95E-10 m/s, 1000 kN.m/m³ energy recorded

Table 3. *Basis Properties of test materials.*

Property	MDD	OMC	LL	PL	PI	SG	%Pass. 0.075 mm	%Pass. 2.35 mm	Color
LS	2.45	17	35	20	15	2.21	30	100	brown
RHA	-	-	-	-	-	2.14	-	100	ash

Table 4. *Chemical oxide wt % composition of LS and RHA by EDXRF analyzer at 40 keV max energy.*

Material	Al_2O_3	SiO_2	Fe_2O_3	CaO	Na_2O	MgO	P_2O_5	TiO_2	MnO	ZnO	SO_3	K_2O
LS	22.10	15.3	10.1	0.62	15.2	4.83	5.7	4.4	10.58	2.2	5.47	3.5
RHA	20.8	57.4	3.27	8.7	0.03	0.74	0.9	0.2	0.4	1.7	1.1	4.8

Table 5. *PCM and pozzolanic condition of the materials and treated specimens.*

Material	PCM			Pozzolanic strength (Al + Si + Fe)
	SM (1.7–2.7)	IM (0.9–1.7)	KH(0.9–1.0)	
LS	1.50	1.02	0.32	47.5%
RHA	2.60	1.63	1.00	81.47%

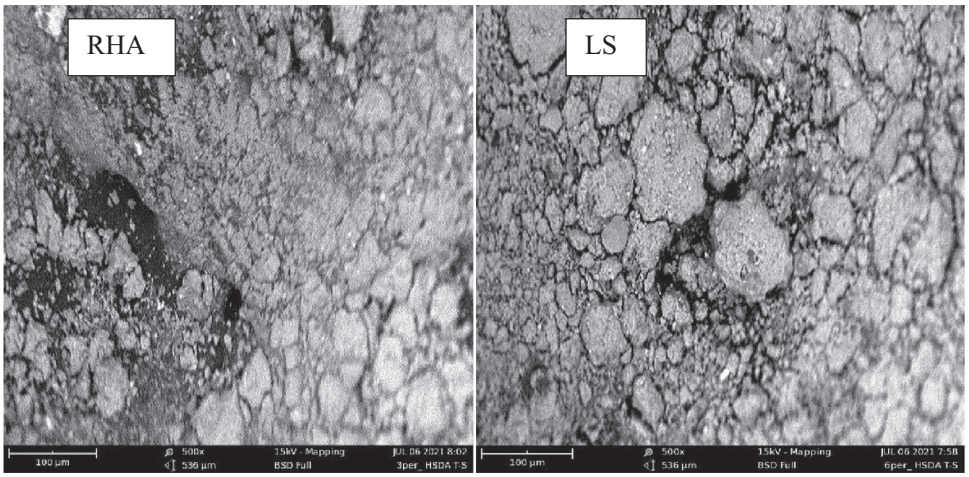

Figure 5. *SEM configuration of RHA and LS.*

50.75E-10 m/s and 2200 kN.m/m^3 energy recorded 32.33E-10 m/s. In Tables 4 and 5, oxide compositions and the PCM of the LS and RHA were presented, which shows the aluminosilicate composition of the soil and ash. These further show the cementing ability of RHA with a PCM of 81.47%, which is above the 70% stipulated by the appropriate design and materials standard for pozzolanas [2, 4]. In Figure 5, the SEM surface configuration of the LS and RHA was presented. It shows the contour differences with LS having the higher and deeper pores, which require pore-filling. The RHA surface contour shows more consistent and compacted fine surface due to its formulation, which agrees with a previous finding by Ashraf *et al.* [1] and Onyelowe *et al.* [21].

3.2 Prediction of hydraulic conductivity

3.2.1 *Model 1: using GP technique*

The developed GP model has six levels of complexity. The population size, survivor size and number of generations were 100 000, 25 000 and 100, respectively. Eq. (1) presented the output formula for (K), while Figure 8(a) shows models fitness. The average errors % of total dataset is 19.6%, while the R^2 value is 0.906. This model shows a considerably high error potential though with a good performance of a little over 90%. It has an advantage of a closed-form equation, which allows the model to be applied manually and this outcome agrees with other GP models previously carried out [11, 22].

$$\frac{K}{10^{10}} = \frac{2.7}{\left(X^{X-1} - 2.17\right)\left(5.8\,X - 1\right)} + 4.33\,X^2\left(X^{X-1} - 1.1\right) - 2.17\,X + ED^{0.372} + 0.372 + Cc^{\left(2.17\,RHA.X - (0.462)^{2.17\,X^2}\right)} \quad (1)$$

where $X = 0.462\,ED.Cc^2$.

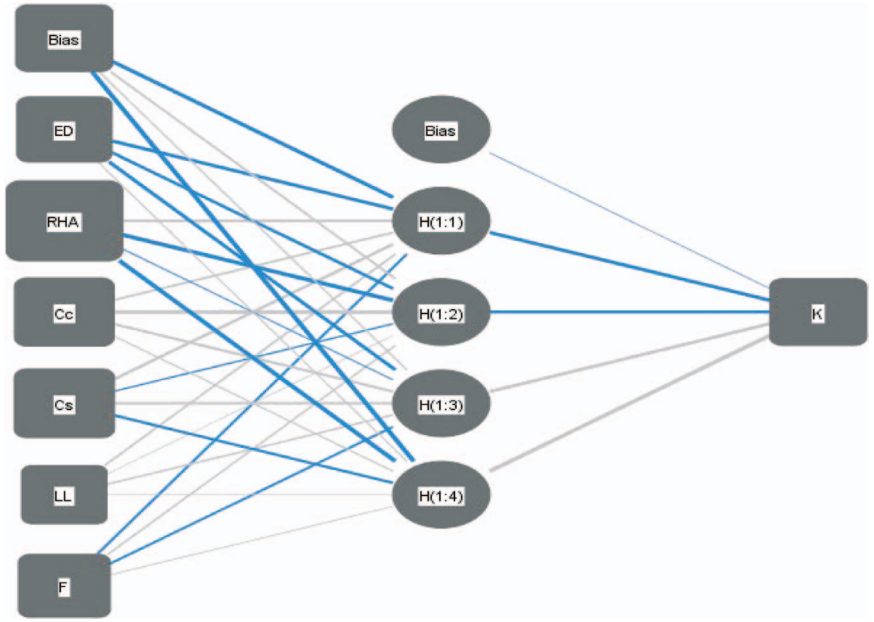

Figure 6. *Architecture of the developed ANN models.*

Table 6. *Weights matrix for the developed ANN-BP model.*

		Hidden layer				Output layer
		H(1:1)	H(1:2)	H(1:3)	H(1:4)	K∗10^{-10}
	(Bias)	−1.622	0.484	0.153	−2.96	
	ED	−1.369	−1.24	−1.37	0.151	
	RHA	1.226	−1.805	−0.148	−2.34	
Input layer	Cc	0.609	1.641	0.876	0.151	
	Cs	1.123	−.287	0.807	−0.933	
	LL	0.392	0.071	0.360	0.077	
	F	−0.763	0.294	−0.760	0.139	
	(Bias)					−0.034
	H(1:1)					−1.393
Hidden layer	H(1:2)					−1.279
	H(1:3)					1.357
	H(1:4)					1.767

3.2.2 *Models 2–4: using ANN technique*

Three models were developed using ANN technique. All the models have the same layout (6:4:1), normalization method (−1.0 to 1.0) and activation function (hyper tan). However, each model utilized different training algorithm as follows: model 2 used the traditional BP algorithm, model (3) used the well-known mathematical algorithm GRG and while model (4) used the famous AI optimization technique GA.

These three developed models were used to predict K values. The used networks layout is illustrated in Figure 6, while the weight matrixes of each model are shown in Tables 6, 7 and 8. The average error % of total dataset are (11.3%, 6.6% and 12.5%) and the R^2 values are 0971, 0.990 and 0.966, respectively. The relative importance values for each input parameter are illustrated in Figure 7, which indicated that RHA dosage is the most important factor, while other factors have much lower influence; this RHA sensitivity index in this research agrees with the studies of Ebid *et al.* [11] and Onyelowe *et al.* [22]. The relations between calculated and predicted values are shown in Figure 8(b–d).

3.2.3 *Model 3: using EPR technique*

Finally, the developed EPR model was limited to quadrilateral level, for six inputs; there are 210 possible terms (126 + 56 + 21 + 6 + 1 = 210) as follows:

$$\sum_{i=1}^{i=6}\sum_{j=1}^{j=6}\sum_{k=1}^{k=6}\sum_{l=1}^{l=6} X_i.X_j.X_k.X_l + \sum_{i=1}^{i=6}\sum_{j=1}^{j=6}\sum_{k=1}^{k=6} X_i.X_j.X_k$$

$$+ \sum_{i=1}^{i=6}\sum_{j=1}^{j=6} X_i.X_j + \sum_{i=1}^{i=6} X_i + C$$

Table 7. *Weights matrix for the developed ANN-GRG model.*

		Hidden layer				Output layer
		H(1:1)	H(1:2)	H(1:3)	H(1:4)	K∗10^{-10}
	(Bias)	−4.65	28.44	−23.47	25.91	
	ED	9.11	29.36	−0.80	25.75	
	RHA	−15.26	66.41	−26.47	23.94	
Input layer	Cc	12.20	45.92	15.88	4.33	
	Cs	−9.58	9.95	−17.51	20.12	
	LL	0.83	−12.36	1.85	−19.12	
	F	3.57	9.59	0.00	16.36	
	(Bias)					−0.47
	H(1:1)					−2.71
Hidden layer	H(1:2)					−0.84
	H(1:3)					3.02
	H(1:4)					0.93

Table 8. *Weights matrix for the developed ANN-GA model.*

		Hidden layer				Output layer
		H(1:1)	H(1:2)	H(1:3)	H(1:4)	K∗10^{-10}
	(Bias)	5.09	21.96	25.68	10.55	
	ED	−8.56	21.25	13.52	6.14	
	RHA	−7.44	18.57	16.38	−6.54	
Input layer	Cc	−7.73	32.09	30.38	6.14	
	Cs	24.59	−11.21	7.58	22.37	
	LL	10.30	−11.24	−4.09	6.03	
	F	−15.85	27.40	−0.84	5.73	
	(Bias)					1.24
	H(1:1)					−2.50
Hidden layer	H(1:2)					−4.00
	H(1:3)					1.67
	H(1:4)					2.02

Table 9. *Summary of the performance accuracies of developed models.*

Technique	Model	SSE	Avg. error %	R^2
GP	Eq. 1	557	19.6	0.906
ANN-BP	Figure 3, Table 3	187	11.3	0.971
ANN-GRG	Figure 3, Table 4	63	6.6	0.990
ANN-GA	Figure 3, Table 5	226	12.5	0.966
EPR	Eq. 2	508	18.7	0.913

The GA technique was applied on these 210 terms to select the most effective 11 terms to predict the values of K. The output is illustrated in Eq. (2) and its fitness is shown in Figure 8(e). The average error % and R^2 values were 18.7% and 0.913, respectively. Finally, the summary of the performance accuracies of the predicted models is presented in Table 9.

$$\frac{K}{10^{10}} = -2.22 + \frac{ED^3.Cc^2.Cs}{3970} - \frac{ED^2.RHA.Cc^3}{15} - \frac{RHA^3}{34.5E6\ Cc^2.Cs} - \frac{28.8\ RHA^2}{ED^2.Cs^2} + \frac{47.RHA^3.Cc}{LL} + \frac{ED.RHA^2.Cs}{7.32E6\ Cc^2} + \frac{ED.Cc^3}{25\ Cs^2} - \frac{RHA}{93\ Cs^3.LL^2} + \frac{LL}{288\ ED.Cc.Cs^2} + \frac{RHA^2.LL^2}{2.75E6\ Cs} \quad (2)$$

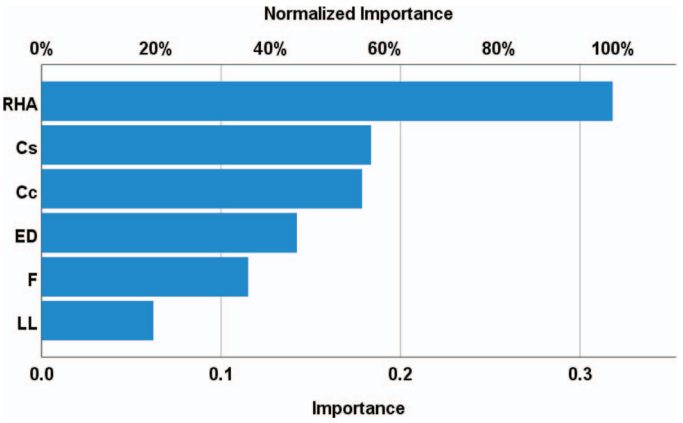

Figure 7. *Relative importance of input parameters.*

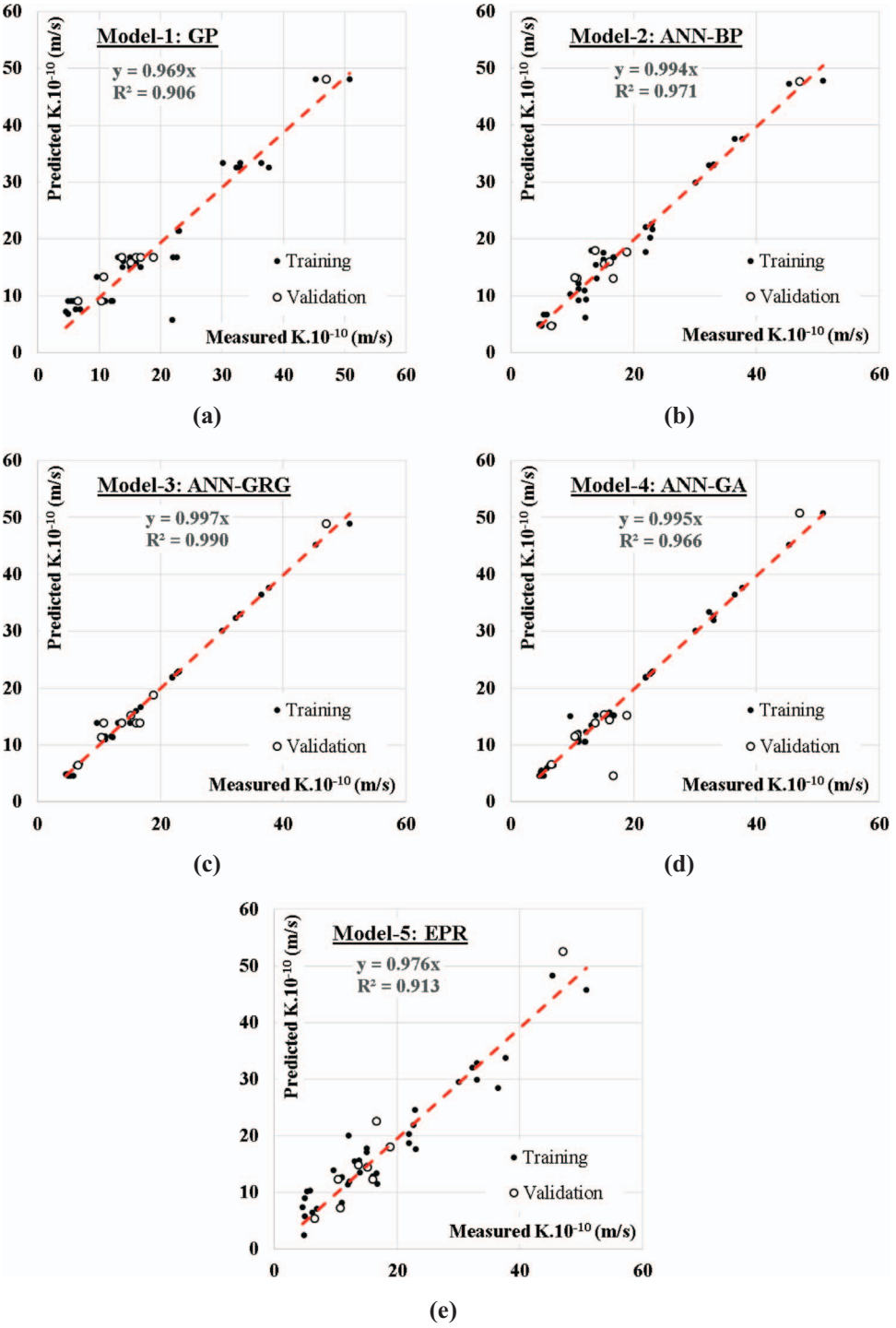

Figure 8. *Relation between predicted and calculated (K) values using the developed models.*

4 CONCLUSIONS

This research presents three models using five AI techniques (GP, ANN-BP, ANN-GRG, ANN-GA and EPR) to predict the hydraulic conductivity (K) in (m/s) using compactive ED in kN.m/m^3, RHA dosage (%), compression index (Cc), swell index (Cs), LL (%) and fines percentage (%) (F).The results of comparing the accuracies of the developed models could be concluded in the following points:

- Both GP and EPR showed almost the same low level of accuracy (80.4% and 81.3%) in order, while the three ANN models presented much better level of accuracy (87.5–93.4%).

- The results indicated that the accuracy of the ANN models is affected by the training algorithm. BP and GA showed almost the same level of accuracy (87.5% & 88.7%), while the GRG showed the best level of accuracy (93.4%).
- Although the prediction accuracy of GP and EPR models are lower than ANN models, their outputs are closed form equations, which could be used manually or as software unlike the ANN output, which cannot be used manually.
- The summation of the absolute weights of each neuron in the input layer of the developed ANN model indicates that RHA dosage had major influences K values and other parameters have less effect on them.
- The developed formulas using GP depended mainly on ED, Cc and RHA, which indicates the minor effect of the other factors on K values. On the other hand, the fine percent (F) did not appear in GP model or EPR model, it has the minimum effect on the K value.
- GA technique successfully reduced the 210 terms of conventional polynomial regression quadrilateral formula to only 11 terms without significant impact on its accuracy.
- Like any other regression technique, the generated formulas are valid within the considered range of parameter values; beyond this range, the prediction accuracy should be verified.

REFERENCES

[1] Ashraf MS, Ghouleh Z, Shao Y. Production of eco-cement exclusively from municipal solid waste incineration residues. *Resour Conserv Recycl* 2019;**149**:332–42.

[2] ASTM C618. 2019. Standard specification for coal fly ash and raw or calcined natural pozzolan for use in concrete. In *American Society for Testing and Materials*. West Conshohocken, PA. ASTM standard C618–19.

[3] ASTM E2809-13. 2013. *Standard Guide for Using Scanning Electron Microscopy/X-Ray Spectrometry in Forensic Paint Examinations*. West Conshohocken, PA: ASTM International.

[4] BS 8615-1. 2019. Specification for pozzolanic materials for use with Portland cement. In *Natural Pozzolana and Natural Calcined Pozzolana*. London: British Standard International.

[5] BS 1377-2, 3. 1990. *Methods of Testing Soils for Civil Engineering Purposes*. London: British Standard Institute.

[6] BS 1924-2 2018 *Hydraulically Bound and Stabilized Materials for Civil Engineering Purposes—Sample Preparation and Testing of Materials During and After Treatment* British Standard Institute London.

[7] Bello Yamusa Y, Alias N, Ahmad K *et al.* Computer modeling approach of leachate flow in compacted laterite soil liner. *MATEC Web of Conferences* 2018;**250**. https://doi.org/10.1051/matecconf/201825001001.

[8] Chompoorat T, Maikhun T, Likitlersuang S. Cement-improved lake bed sedimentary soil for road construction. *Proc Ins Civil Eng Ground Improv* 2019;**172**:192–201.

[9] de Silva GHMJS, Surangi MLC. Effect of waste rice husk ash on structural, thermal and run-off properties of clay roof tiles. *Constr Build Mater* 2017;**154**:251–7.

[10] Eberemu AO, Yohanna P, Aliyu M, Abdu-Aguye A. Consolidation characteristics of lateritic soil treated with rice husk ash. *Malaysian J Civ Eng* 2022;**34**:19–28.

[11] Ebid AM, Onyelowe KC, Arinze EE. Estimating the ultimate bearing capacity for strip footing near and within slopes using AI (GP, ANN, and EPR) techniques. *J Eng* 2021;**2021**:3267018. https://doi.org/10.1155/2021/3267018.

[12] Emmanuel E, Anggraini V, Gidigasu SSR. A critical reappraisal of residual soils as compacted soil liners. *SN Appl Sci* 2019;**1**:460. https://doi.org/10.1007/s42452-019-0475-7.

[13] Farias JP, Loebens L, Demarco CF *et al.* Post-treatment of landfill leachate using rice husk ash as adsorbent medium. *Rev Ambiente Agua* 2019;**14**. https://doi.org/10.4136/ambi-agua.2350.

[14] Ghosh S, Mukherjee S, Sarkar K *et al.* Experimental study on chromium containment by admixed soil liner. *J Environ Eng* 2012;**138**:1048–57.

[15] Giroud JP, Badu-Tweneboah K, Soderman KL. Comparison of leachate flow through compacted clay liners in landfill liner systems. *Geosynth Int* 1997;**4**:391–431.

[16] Ige OO. Note on liners for containment of Leachate in sanitary landfills to enhance sustainable environment. *Int J Dev Sustain* 2013;**2**:380–9.

[17] Kumar A, Gupta D. Behavior of cement-stabilized fiber-reinforced pond ash, rice husk ash-soil mixtures. *Geotext Geomembr* 2016;**44**:466–74.

[18] Muntohar AS, Widianti A, Hartono E, Diana W. Engineering properties of silty soil stabilized with lime and rice husk ash and reinforced with waste plastic fiber. *J Mater Civ Eng* 2013;**25**:1260–70.

[19] Nayanthika IVK, Jayawardana DT, Bandara NJGJ *et al.* Effective use of iron-aluminum rich laterite based soil mixture for treatment of landfill leachate. *Waste Manag* 2018;**74**:347–61.

[20] Ojuri O, Oluwatuyi O. Strength and hydraulic conductivity characteristics of sand-bentonite mixtures designed as a landfill liner. *Jordan J Civ Eng* 2017;**11**.

[21] Onyelowe KC, Tome S, Ebid AM *et al.* Effect of desiccation on ashcrete (HSDA)-treated soft soil used as flexible pavement foundation; zero carbon stabilizer approach. *Int J Low Carbon Technol* 2022;**17**:563–70.

[22] Onyelowe KC, Ebid AM, Onyia ME, Nwobia LI. Predicting nanocomposite binder improved unsaturated soil UCS using genetic programming. *Nanotechnol Environ Eng* 2021;**6**:39. https://doi.org/10.1007/s41204-021-00134-z.

[23] Onyelowe KC, Bui Van D, Ubachukwu O *et al.* Recycling and reuse of solid wastes; a hub for ecofriendly, ecoefficient and sustainable soil, concrete, wastewater and pavement reengineering. *Int J Low Carbon Technol* 2019;**14**:440–51.

[24] Ordoñez Muñoz Y, dos Santos L, Izzo R *et al.* The role of rice husk ash, cement and polypropylene fibers on the mechanical behavior of a soil from Guabirotuba formation. *Transp Geotech* 2021;**31**:100673. https://doi.org/10.1016/j.trgeo.2021.100673.

[25] S., N. A, Anh LH, Thanh NT *et al.* Life cycle assessment of substitutive building materials for landfill capping systems in Vietnam. *Appl Sci* 2022;**12**:3063. https://doi.org/10.3390/app12063063.

[26] Santos A, Fernández J, Guadaño J *et al.* Chlorinated organic compounds in liquid wastes (DNAPL) from lindane production dumped in landfills in Sabiñanigo (Spain). *Environ Pollut* 2018;**242**:1616–24.

[27] Suksiripattanapong C, Kua T-A, Arulrajah A *et al.* Strength and microstructure properties of spent coffee grounds stabilized with rice husk ash and slag geopolymers. *Constr Build Mater* 2017;**146**:312–20.

[28] Thankam NS, Rekha V, Shankar U. Use of lateritic soil amended with bentonite as landfill liner. *Rasayan J Chem* 2017;**10**. https://doi.org/10.7324/RJC.2017.1041818.

[29] Umar SY, Elinwa AU. Evaluation of the hydraulic conductivity of compacted laterite-metakaolin mixtures for solid waste leachate containment. *FUOYE J Eng Technol* 2020;**5**. https://doi.org/10.46792/fuoyejet.v5i1.476.

[30] Yamusa YB, Ahmad K, Rahman NA. Sustainable design of compacted laterite soil liner. *GCEC 2017* 2019a;**9**. https://doi.org/10.1007/978-981-10-8016-6_84.

[31] Yamusa YB, Ahmad K, Rahman NA *et al.* Volumetric shrinkage of compacted soil liner for sustainable waste landfill. *Chem Eng Trans* 2018;**63**. https://doi.org/10.3303/CET1863103.

[32] Yamusa YB, Alias N, Ahmad K *et al.* Engineering characteristics of compacted laterite soil as hydraulic barrier in waste containment application. *J Eng Sci Technol* 2020;**15**.

[33] Yamusa YB, Sa'ari R, Ahmad K *et al.* Monitoring leachate migration in compacted soil using digital image technique. *Eng Technol Appl Sci Res* 2019b;**9**:3685–91.